06,10

Structure and influence of pressure on low-temperature dielectric properties of nanocomposites based on mesoporous glasses containing $K_{(1-x)}(NH_4)_xH_2PO_4$

© O.A. Alekseeva[1], E.V. Bogdanov[2], M.S. Molokeev[2], A.A. Naberezhnov[1], A.A. Sysoeva[1]

[1] Ioffe Institute,
St. Petersburg, Russia
[2] Kirensky Institute of Physics, Federal Research Center KSC SB, Russian Academy of Sciences,
Krasnoyarsk, Russia

E-mail: alekseeva.oa@mail.ioffe.ru

Received April 2, 2025
Revised April 24, 2025
Accepted April 30, 2025

The results of a study of the structure and influence of pressure on the dielectric response of nanocomposite materials based on mesoporous glass with an average pore diameter of 7(2) nm containing solid solutions of $(K_{(1-x)}(NH_4)_xH_2PO_4$ with $x = 0.05$, 0.1 and 0.15) introduced into the pore space are presented. It is shown that in nanocomposites with $x = 0.1$ and 0.15 tetragonal and monoclinic phases coexist. For the composition with $x = 0.05$, the phase diagram $T_C(P)$ was obtained and the coefficient $dT_C/dP \approx -2.5(2)$ was determined. In nanocomposites with $x = 0.05$ and 0.15 at $P = 0$, an increase in the ferroelectric phase transition temperature T_C is observed compared to similar bulk materials.

Keywords: ammonium potassium dihydrogen phosphate, nanocomposite materials, X-ray diffraction, dielectric response.

DOI: 10.61011/PSS.2025.05.61494.67-25

1. Introduction

Ferroelectric materials from the KH_2PO_4 (KDP) family are of great interest in terms of nonlinear optics applications and for creation of optical modulators, while large crystals with good optical quality can be easily grown from a water solution. At room temperature, KDP is paraelectric (PE) with tetragonal symmetry (space group $I\bar{4}2d$) and transforms into an orthorhombic ($Fdd2$) ferroelectric (FE) phase at $T_C \approx 123$ K. This phase transition is of the order-disorder type, spontaneous polarization results from an opposite ionic displacement of K^+ and $(PO_4)^{3-}$ due to electron density redistribution in a plane perpendicular to the displacement axis, with proton ordering on O−H...O hydrogen bonds in the FE phase playing the main role [1]. $NH_4H_2PO_4$ (ADP) is also included in the KDP family, but is an antiferroelectric material. At room temperature, ADP also has a tetragonal lattice, and the structure becomes rhombic below the phase transition point ($T_N \approx 147$ K). Antiferroelectric phase transition (AFE-PT) is considered to be associated with proton ordering on the O−H...O bonds [2,3]. ADP forms a continuous series of solid solutions with KDP; phase diagrams [4–6] and properties [2,3,7] of $K_{1-x}(NH_4)_xH_2PO_4$ (KADP) compounds are well understood. In KADP solid solutions, these phase transitions are suppressed due to accidental substitution of the K^+ ions with $(NH_4)^+$ groups resulting in occurrence of a dipole glass phase in these compounds during cooling in a quite wide concentration range ($x = 0.22-0.67$) due to a competition between the ferroelectric and antiferroelectric ordering [4,5,8]. At low temperatures and ammonia concentrations of $0.22 < x < 0.67$, physical property anomalies are observed and occur due to freezing of dipole moments in transition to the proton glass (PG) phase. Review of these structural surveys of compounds with intermediate ammonia concentrations showed that there was a short-range order in the atom arrangement at low temperatures. Studies [4–6,8] show that the boundaries between FE, PE and AFE regions on the phase diagrams are diffused and have a form of extended concentration regions, within which the PE, FE and PG phases (left boundary of the phase diagram) and PE, PG and AFE phases (right boundary) exist. It was also found that there was a dramatic decrease in the FE transition temperature in the low ammonia concentration region as the fraction of ADP increased, and the transition itself became greatly smeared [9]. A quite large decrease in the PT temperatures when external pressure is applied is another distinguishing feature of KDP and ADP: at the initial stage (at low pressures), a linear law with inclinations $dT_C/dP \approx -4.5$ K/kbar for KDP and $dT_N/dP \approx -3.4$ K/kbar for ADP is adequately fulfilled [10]. As the pressure increases, dT_C/dP and dT_N/dP deviate from the linear law and become sharper. In KDP, the PE−FE phase transition disappears at a pressure higher than 17 kbar, and in ADP, the PE−AFE phase transition is not observed any longer at $P \geq 34$ kbar.

The influence of limited geometry conditions on phase transition in KDP, ADP and KADP was studied before for nanocomposite materials (NCM) made on the basis of mesoporous glass with a mean pore diameter [11–20], artificial opals [11], chrysotile asbestoses [21] and MCM-41 type mesoporous molecular sieves [20,22]. Despite some inconsistency of the available quantitative data, in particular comparing with earlier results, it is suggested that the limited geometry conditions lead to an increase in PT temperatures in NCM with KDP, but no regular dependence on the mean matrix pore diameter was observed. As for NCM with ADP, decrease in the AFE-PT temperature was observed [13] for porous glass nanocomposite materials as the pore radius deceases from 160 to 23 nm. Dielectric properties of nanocomposite materials based on porous glass with a mean pore diameter of 45(5) nm that contain $K_{1-x}(NH_4)_xH_2PO_4$ (KADP) solid solutions introduced into the pore volume with $x = 0.05$, 0.1 and 0.15 (in molar percent) were studied on heating and cooling in [16,17], and it was shown that the ADP impurity in these NCM's causes significant increase in the PE−FE transition temperature compared with the equivalent KADP bulk solid solutions. The observed anomalies in phase transition temperature behavior for NCM with KDP, ADP and KADP are quite logically associated with the influence of elastic stresses at the „matrix–embedded material" interface [12,16–18,20] that occur due to a large difference in thermal expansion coefficients (TEC) of the matrix and embedded material. Indeed, for ADP $\alpha_1 \approx$ $\approx (34.0-39.3)\cdot 10^{-6}\,K^{-1}$ and $\alpha_3 \approx (1.9-5.3)\cdot 10^{-6}\,K^{-1}$ in the temperature range of 203−407 K, and for KDP within 123−363 K $\alpha_1 \approx (20-6.6)\cdot 10^{-6}\,K^{-1}$ and $\alpha_3 \approx$ $\approx (34.3-44.6)\cdot 10^{-6}\,K^{-1}$ [23], while for the Vicor® mesoporous glass, TEC is equal to $\sim 7.5\cdot 10^{-7}\,K^{-1}$ within 273−573 K [24,25], i. e. much lower than for materials embedded into the pore volume. Thus, it may be expected that an externally applied pressure will affect significantly the PE−FE phase transition in NCM containing embedded KADP solid solutions; but such studies haven't been carried out before. Features of the crystal structure of NCM based on mesoporous glasses with small mean pore diameters (7 nm in this case) containing the above-mentioned KADP solid solutions haven't been studied either. The objective of this work has been to fill the above-mentioned gaps using X-ray diffraction and survey of temperature behavior of the KADP dielectric response when external pressure is applied to a sample.

2. Samples and experimental techniques

Samples were prepared using alkaline-borosilicate glasses with a mean pore diameter of 7(2) nm (hereinafter referred to as PG7) made in the Ioffe Institute using a standard process [26]. The average pore diameter was determined using mercury porosimetry data. Empty pore volume in the samples was 25.5 % of the total sample volume. Pores in these glasses form a multiply-connected (dendritic) three-dimensional system of through channels. Thin (0.6−0.7 mm) rectangular PG7 plates were used for filling, for which they were immersed into a hot ($\sim 70^\circ$C) saturated $K_{1-x}(NH_4)_xH_2PO_4$ water solution and held for ~ 1 h. Note that the Curie temperature T_C in $(1-x)$KDP-(x)ADP solid solutions in low ADP concentration region depends greatly on the molar concentration (x) ADP: $dT_C/dx \approx -250$ K [27]. Determination accuracy of the molar content of solution components was at least 1 %; thus, a possible PT temperature shift resulting from determination inaccuracy of solid solution composition was not higher than 2−3 K. Three types of samples were fabricated. PG7+KADP5, PG7+KADP10 and PG7+KADP15 with 5, 10 and 15 mol.% of the ADP impurity, respectively. The filling procedure was repeated three times to increase the volume of material embedded into the material pores. Further, the samples were dried at $\sim 100^\circ$C for 4−6 h, then their surface was cleaned thoroughly to remove all possible remaining bulk material. Pore volume filling percentage was determined from the sample weighing results before and after KADP introduction and was about 50 % for PG7+KADP5, 25.5 % for PG7+KADP10 and 36 % for PG7+KADP15. The same procedure was also used to make a PG7+KDP reference sample.

Structural qualification of all prepared samples used X-ray diffraction on the Haoyuan DX-2700BH powder diffractometer provided by the Krasnoyarsk Regional Center of Research Equipment of Federal Research Center „Krasnoyarsk Science Center SB RAS") on the Cu$K\alpha$ line. Diffractometer's instrumental resolution function was determined from the scattering data on a silicon powder sample. All structural surveys were conducted at room temperature. Results were processed in dedicated Topaz software installed on the diffractometer and FullProf profile analysis package [28].

Dielectric response to external hydrostatic pressure was measured using the E7-20 LCR meter at 1 kHz on heating at a rate of about 0.5−2 K/min. Silver electrodes were deposited on the prepared samples to which 0.1 mm copper wires were attached using conductive adhesive. Pressure was measured using a resistance pressure gage in the form of a coil made of 0.05−0.1 mm aged manganin wire. The manganin pressure gauge was chosen because its resistance increases linearly with pressure growth up to ~ 1.5 GPa (15 kbar) and it has a negligible temperature resistance coefficient. The pressure gauge was calibrated by resistance measurement at atmospheric pressure. Reproducibility was verified in hydrostatic pressure increase and decrease conditions. Pressure up to 0.5 GPa was built up in a cylinder–piston type chamber connected to a multiplier; transformer oil or pentane (or mixtures thereof) were used as a pressure transfer fluid depending on the studied temperature region. Sample temperature was measured using a copper–konstantan thermocouple that gives an error of ~ 0.3 K in the 100−400 K measurement range. Data was

Comparison of lattice cell parameters determined in this work with those known for monoclinic KDP(DKDP) structures with space group $P2_1$

Sample	a, Å	b, Å	c, Å	β, deg	Comments
PG7+KADP10	7.37(3)	14.24(3)	7.16(3)	92.5(2)	This study
PG7+KADP15	7.41(2)	14.20(3)	7.11(2)	92.7(1)	HThis study
PG7+KDP	7.335(2)	14.551(4)	7.009(2)	92.98(2)	From [30]
PG7+DKDP	7.464(3)	14.656(6)	7.068(4)	92.66(3)	Highly deuterated KDP [31]
KDP single crystal	7.44(8)	14.518(1)	7.602(5)	103.107(7)	From [32]
DKDP single crystal	7.45(1)	14.71(2)	7.14(1)	92.31(1)	Highly deuterated KDP [29]

collected using an analog-to-digital converter. Measurement accuracy was ± 1 K for temperature and ± 10 MPa for pressure.

3. Results and discussion

3.1. X-ray diffraction

Figure 1, *a* and *b* shows X-ray diffraction patterns recorded for the PG7+KADP5 and PG7+KADP15 samples.

Crystal structure of the PG7+KDP and PG7+KADP5 samples (Figure 1, *a*) is adequately described by the tetragonal phase known for KDP with space group $I\bar{4}2d$, and the elastic peak width is fully determined by the diffractometer's instrumental resolution. Diffraction pattern or all samples have an intense background from scattering of amorphous SiO_2 that composes the matrix skeleton. As can be clearly seen in Figure 1, *b*, increase in the ADP content causes distortion of the line shape of the most intense peak (200) of the tetragonal phase and occurrence of additional peaks that are clearly observed, for example, in the scattering angle region $2\theta = 26.7-28°$. Simulation in the profile-matching mode has shown that these additional peaks adequately match the monoclinic phase $P2_1$observed previously [19,29](lower vertical bar row in Figure 1, *b*), and the present distortion (broadening) of the tetragonal phase reflection (200) observed for NCM PG7+KADP10 and PG7+KADP15 was caused by the peak (200) from the monoclinic phase at the near 2θ.

For detailed comparison of line shape distortion of this elastic peak of the tetragonal phase see Figure 2, *a* and *b*. The figure clearly shows that the width of peak (200) of this phase fully corresponds to the resolution function (dashed line) as mentioned above. Note also that the relative contribution of the monoclinic phase grows as the ADP concentration increases. Unfortunately, lack of statistics prevented us from performing a full profile analysis taking into account the two-phase state of PG7+KADP10 and PG7+KADP15 NCM, but the „profile-matching mode" procedure was used to estimate the monoclinic phase lattice cell parameters.

Figure 3 shows the dependences of lattice cell parameters a and c for the tetragonal phase for all NCM. Observed

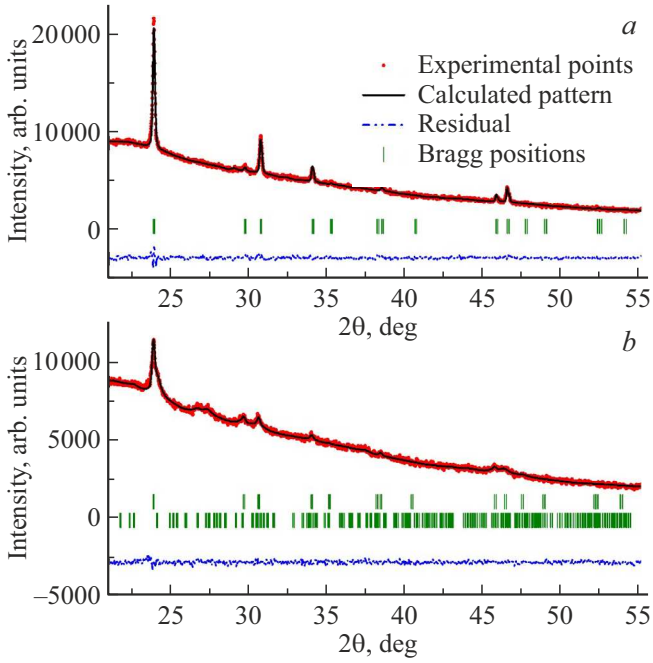

Figure 1. Diffraction patterns for the PG7+KADP5 (*a*) and PG7+KADP15 (*b*) samples. Red points — experiment, solid black line — matching, green bars— elastic peak positions, solid blue lines at the bottom (*a*) and (*b*) — „experiment–matching" residual.

growth of these parameters with an increase in the ADP concentration corresponds closely to the known trend for bulk KADP [4]. The table shows quite rough estimates (due to lack of statistics) of lattice constants obtained for the monoclinic phase observed in PG7+KADP10 and PG7+KADP15 compared with the literature data.

Based on the known diffractometer's resolution function and using the elastic peak lineshape distortion analysis algorithm in the presence of two-phase state of the test samples [30], the lower size limit of the coherent scattering region (CSR) was estimated for the tetragonal phase regions and was about 100−130 nm. In addition, the CSR size was determined for the monoclinic phase in PG7+KADP15: $\langle D \rangle \approx 15$ nm. Any reliable estimate of the CSR size for this phase was not possible for PG7+KADP10 due to low intensity of the corresponding peaks.

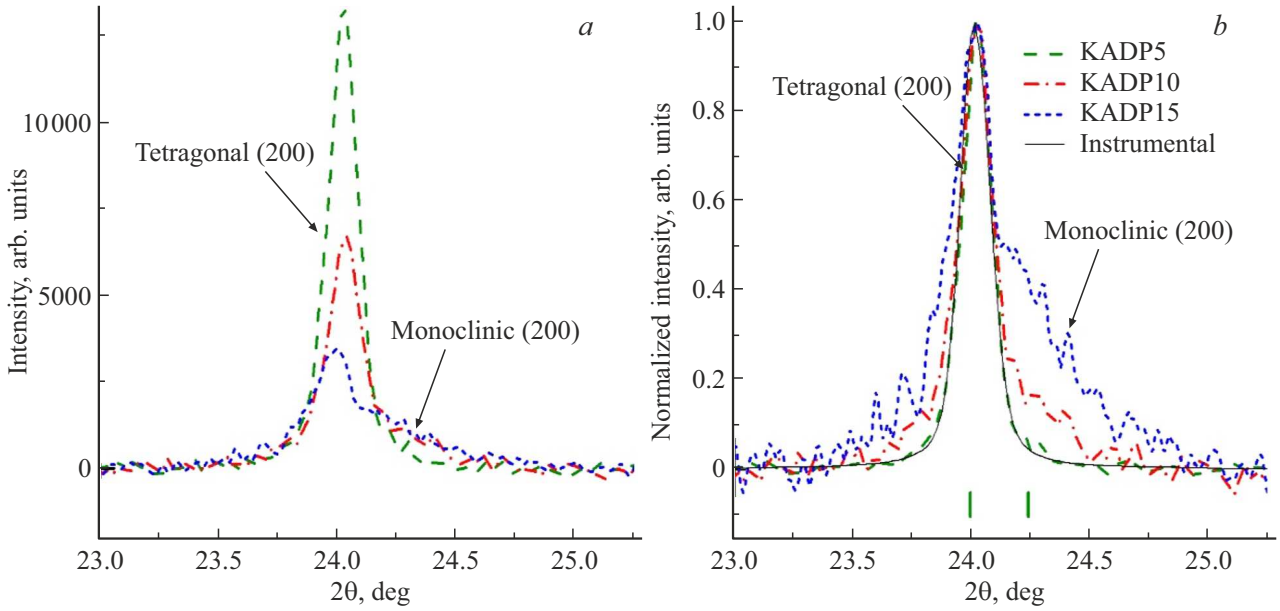

Figure 2. Evolution of the tetragonal phase reflection lineshape (200) as the ADP concentration increases: *a* — initial data, *b* — normalized to maximum. Green dashed line — PG7+KADP5, red dash-dotted line — PG7+KADP10, blue dotted line — PG7+KADP15. Solid black line in Figure (*b*) — is the instrumental resolution. Background from amorphous SiO2 was subtracted. Green bars at the bottom of Figures (*a*) and (*b*) — are positions of elastic peaks (200) for the tetragonal and monoclinic phases.

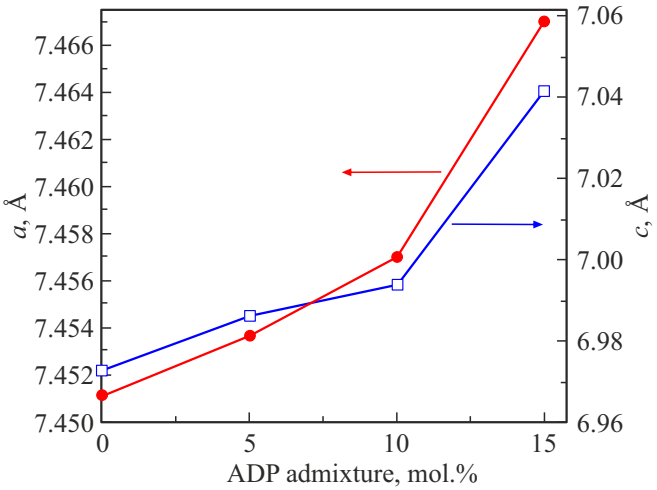

Figure 3. Dependence of tetragonal phase lattice cell parameters vs. the ADP impurity concentration in PG7+KADP NCM. Errors do not exceed the symbol size.

3.2. Pressure influence on the dielectric response of nanocomposite materials

Figure 4 shows temperature dependences of permittivity ε at several pressure positions for PG7+KADP5 NCM. The figure clearly shows that the increase in pressure leads to occurrence of an explicitly observed anomaly (peak) in $\varepsilon(T)$, that may correspond to the PE−FE phase transition because previous dielectric response surveys of unfilled mesoporous glasses of this type [33] have shown that there were no any anomalies in this temperature range in $\varepsilon(T)$ either on heating or on cooling.

Position of maximum for the PG7+KADP5 sample shifts towards lower temperatures as the pressure grows (P), while the peak width decreases, i. e. it becomes more clearly pronounced. The inset in the figure shows $T_C(P)$ for this sample. Assuming that this dependence is linear at low ADP concentrations and low pressures (as it was shown for bulk KDP and ADP in [10]),

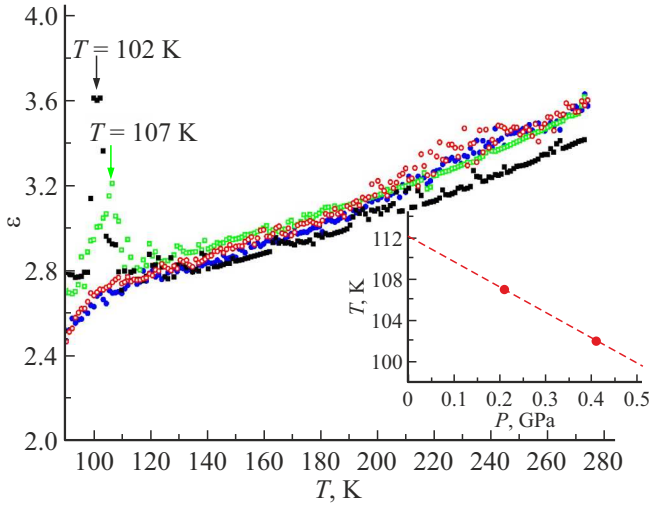

Figure 4. Temperature dependence of permittivity for PG7+KADP5 at $P = 0$ GPa — empty blue and red circles, $P = 0.2$ GPa — empty green boxes and $P = 0.41$ GPa — black boxes. Inset — phase diagram$T(P)$.

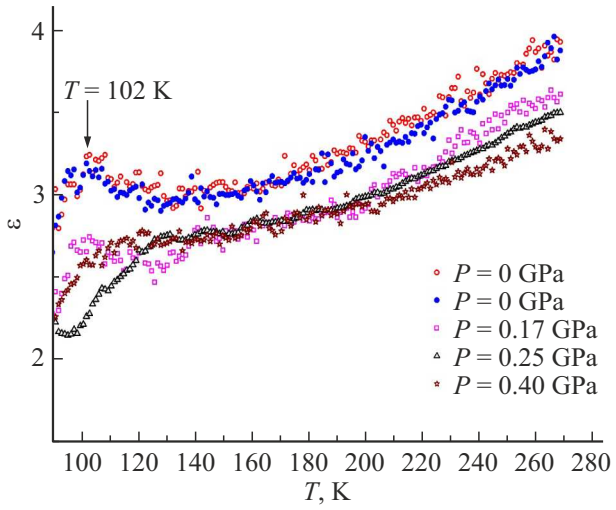

Figure 5. Temperature dependence of permittivity for PG7+KADP15 at $P = 0$ GPa — empty blue and red circles, $P = 0.17$ GPa — pink boxes, $P = 0.25$ GPa — black triangles and $P = 0.4$ GPa — brown asterisks.

$T_C(P = 0) \approx 112(1)$ K and $dT_C/dP \approx -2.5(2)$ K/kbar may be estimated for PG7+KADP5 NCM.

As for the absence of a clear peak $\varepsilon(T)$ at $P = 0$ at 112 K, Figure 4 actually shows that there is a greatly smeared anomaly in $\varepsilon(T)$ in the temperature region below 140 K and up to 100 K, that probably corresponds to the phase transition. Such behavior of $\varepsilon(T)$ (strong expansion of a region corresponding to PT implementation) at $P = 0$ in the PT region for NCM based on glasses with large average pore diameter, in which similar KADP solid solutions were introduced, was observed in [16,17].

Figure 5 shows $\varepsilon(T)$ for PG7+KADP15 NCM at $P = 0, 0.17, 0.25$ and 0.4 GPa. Here, note that there is a greatly smeared anomaly in the absence of applied pressure in the temperature range of 95−120 K with a maximum at 102 K, while the shape and position of the maximum remained almost unchanged for two successive measurement runs. It is suggested that this greatly broadened peak at $P = 0$ corresponds to the FE−PE phase transition because an increase in pressure leads to suppression of this anomaly, and this is what should have been observed at $dT_C/dP < 0$. Anomaly maximum in $\varepsilon(T)$ is at $T_C \sim 102$ K. For PG7+KADP10 NCM, no any explicit anomaly was found in $\varepsilon(T)$ when pressure was applied, which was probably caused by insufficient filling of the pore volume with the embedded material. Thus, the dielectric spectroscopy data indicates that restricted geometry conditions without external pressure lead to sharp change in the inclination of the PE and FE phase boundary in PG7+$K_{1-x}(NH_4)_xH_2PO_4$ NCM at low ADP concentrations compared with bulk materials.

Indeed, for bulk $K_{0.95}(NH_4)_{0.05}H_2PO_4$, T_C is ~ 104 K, and for $K_{0.85}(NH_4)_{0.15}H_2PO_4$, $T_C \approx 69$ K (according to [4,5,9]); while for PG7+KADP5 NCM, $T_C \approx 112$ K, and for PG7+KADP15, $T_C \approx 102$ K according to our estimates. Also note that the transition is still very smeared at $P = 0$. Pressure application leads to a decrease in T_C in PG7+KADP5 NCM, while the temperature region, where PT occurs, narrows as the pressure increases. dT_C/dP remains negative as in bulk KDP and ADP.

4. Conclusion

Comprehensive surveys of structure and pressure influence on dielectric properties of NCM based on mesoporous glasses with a mean pore diameter of 7 nm containing $K_{(1-x)}(NH_4)_xH_2PO_4$ with $x = 0.05, 0.1$ and 0.15 introduced from a saturated water solution. It was found that two phases co-exist in the PG7+KADP10 and PG7+KADP15 nanocomposites at room temperature: the main tetragonal (space group $I\bar{4}2d$) and an admixture of minor monoclinic phase (group $P2_1$ is more probable). Increase in ADP concentration in these NCM's leads to a growth of both relative fraction of the monoclinic phase and tetragonal phase lattice cell parameters. Monoclinic phase lattice parameters were estimated for PG7+KADP10 and PG7+KADP15 NCM. Temperature dependence of phase transition on pressure for the PG7+KADP5 nanocomposite and phase diagram T_C *vs* P were plotted from the dielectric response analysis. Parameter $dT_C/dP \approx -2.5(2)$ K/kbar was determined for this NCM and is much lower than that for bulk KDP and ADP. It is shown that the restricted geometry conditions without external pressure and at low ADP concentrations lead to an increase in phase transition temperatures in NCM with KADP compared with those in bulk materials.

Acknowledgments

The authors would like to express gratitude to the Krasnoyarsk Regional Center of Research Equipment of Federal Research Center „Krasnoyarsk Science Center SB RAS“ for the assistance in structural surveys.

Conflict of interest

The authors declare that they have no conflict of interest.

References

[1] D.S. Bystrov, E.A. Popova. Ferroelectrics **72**, *1*, 147 (1987).
[2] M. Lines, A. Glass. Principles and Applications of Ferroelectrics and Related Materials. Oxford Univ. Press (1977). 680 p.
[3] G.A. Smolensky, V.A. Bokov, V.A. Isupov, N.N. Kraynik, R.E. Pasynkov, M.S. Shur. Segnetoelektriki i antisegnetoelektriki. Nauka, L. (1971). 476 s. (in Russian).
[4] Y. Ono, T. Hikita, T. Ikeda. J. Phys. Soc. Jpn **56**, *2*, 577 (1987).
[5] S.A. Gridnev, L.N. Korotkov, S.P. Rogova, L.A. Shuvalov, R.M. Fedosjuk. Ferroelectr. Lett. Sect. **13**, *3*, 67 (1991).
[6] O.J. Kwon, J.-J. Kim. Phys. Rev. B **48**, *9*, 6639 (1993).
[7] R. Blinc, B. Žekš. Soft Modes in Ferroelectrics and Antiferroelectrics. North-Holland Publishing Company (1974). 317 p.

[8] T.N. Korotkova, L.N. Korotkov, L.A. Shuvalov, R.M. Fedosyuk. Crystallogr. Rep. **41**, *3*, 477 (1996).
[9] L.N. Korotkov, L.A. Shuvalov, R.M. Fedosyuk. Ferroelectrics **265**, *1*, 99 (2002).
[10] G.A. Samara. Phys. Rev. Lett. **27**, *2*, 103 (1971).
[11] E.V. Colla, A.V. Fokin, E.Yu. Koroleva, Yu.A. Kumzerov, S.B. Vakhrushev, B.N. Savenko. NanoStructured Mater. **12**, *5–8*, 963 (1999).
[12] V. Tarnavich, L. Korotkov, O. Karaeva, A. Naberezhnov, E. Rysiakiewicz-Pasek. Optica Applicata **40**, *2*, 305 (2010).
[13] T. Marciniszyn, R. Poprawski, J. Komar, A. Sieradzki. Phase Transitions **83**, *10–11*, 909 (2010).
[14] A. Cizman, T. Marciniszyn, E. Rysiakiewicz-Pasek, A. Sieradzki, T.V. Antropova, R. Poprawski. Phase Transitions **86**, *9*, 910 (2012).
[15] E. Koroleva, A. Naberezhnov, A. Sysoeva, P. Vanina, V. Nizhankovskii. Tech. Phys. Lett. **41**, *10*, 981 (2015).
[16] P.Yu. Vanina, A.A. Naberezhnov, O.A. Alekseeva, A.A. Sysoeva, D.P. Danilovich, V.I. Nizhankovskii. Nanosystems: Phys., Chem., Math. **8**, *4*, 535 (2017).
[17] P.Yu. Vanina, A.A. Naberezhnov, A.A. Sysoeva, V.I. Nizhankovskii, B. Nacke. Nanosystems: Phys., Chem., Math. **8**, *6*, 835 (2017).
[18] V.V. Tarnavich, A.S. Sidorkin, T.N. Korotkova, E. Rysiakiewicz-Pasek, L.N. Korotkov, N.G. Popravko. Crystals **9**, *11*, 593 (2019).
[19] O.A. Alekseeva, M.O. Enikeeva, A.A. Naberezhnov, A.A. Sysoeva. Tech. Phys. Lett. **50**, *6*, 5 (2024).
[20] N.I. Uskova, D.Yu. Podorozhkin, E.V. Charnaya, S.V. Baryshnikov, A.Yu. Milinskiy, D.Yu. Nefedov, A.S. Bugaev, M.K. Lee, L.J. Chang. Ferroelectrics **514**, *1*, 50 (2017).
[21] Y.A. Kumzerov, N.F. Kartenko, L.S. Parfen'eva, I.A. Smirnov, A.V. Fokin, D. Wlosewicz, H. Misiorek, A. Jezowski. Phys. Solid State **53**, *5*, 1099 (2011).
[22] A.Yu. Milinskiy, S.V. Baryshnikov, E.V. Charnaya. Ferroelectrics **501**, *1*, 109 (2016).
[23] A.A. Blistanov, V.S. Bondarenko, N.V. Perelomova, F.N. Strizhevskaya, V.V. Chkalova, M.P. Shaskolskaya. Akusticheskie kristally. Nauka, M. (1982). 632 p. (in Russian).
[24] Precision in Glass & Optics for over 25 Years, VYCOR® 7913 High-temperature glass with 96% SiO_2 content, https:/www.pgo-online.com/intl/vycor.html (Accessed: 20 August 2024).
[25] M.E. Nordberg. J. Am. Ceram. Soc. **27**, *10*, 299 (1944).
[26] O.V. Mazurin, E.A. Porai-Koshits. Phase Separation in Glass. North-Holland, Amsterdam (1984). 369 p.
[27] B.-K. Choi, J.-J. Kim. Phys. Rev. B **28**, *3*, 1623 (1983).
[28] FullProf suite. https://www.ill.eu/sites/fullprof/ (2024). (Accessed 4 August 2024)
[29] T. Fukami, R.-H. Chen. J. Phys. Soc. Jpn *75*, *7*, 074602 (2006).
[30] O.A. Alekseeva, A.A. Nabereznov, G.-I. Ekosse. Tech. Phys. **67**, *9*, 1265 (2022).
[31] B. Dorner, I. Golosovsky, Yu. Kumzerov, D. Kurdyukov, A. Naberezhnov, A. Sotnikov, S. Vakhrushev. Ferroelectrics **286**, *1*, 213 (2003).
[32] R. Nelmes. Physica Status Solidi B **52**, *2*, K89 (1972).
[33] N.I. Porechnaya. Strukturnye osobennosti i svoistva dvukhfaznykh zhelezosoderzhashchikh kompositnykh matrits na ikh osnove. Kand. diss.k.f.-m.n. SPbGPY, S.-Peterburg (2013). p. 123. (in Russian).

Translated by E.Ilinskaya